A Reflecting/Absorbing Dual-Mode Textile Metasurface Design

Menglin Zhai, Tian Zhang, Rui Pei, Mark Leach, Eng Gee Lim, *senior member*, *IEEE*, Zhao Wang, Jingchen Wang, Qiang Hua, Mobayode Akinsolu, Bo Liu, *senior member*, *IEEE*, and Yi Huang, *fellow*, *IEEE*

***Abstract*—A textile-based reflecting/absorbing dual-mode metasurface is proposed in this paper. For the reflecting mode of the design, a conventional square patch electromagnetic band gap (EBG) structure is adopted and the zero-degree refection phase center is tuned to 2.4 GHz. For the absorbing mode, a carbon-coated resistive net is applied on top of the EBG patches to redirect the current flow at resonance and hence achieve energy dissipation with the resistance. The underlying reconfigurable logic is analyzed with a dispersion diagram, surface current distribution, and equivalent circuit/impedance matching analysis. By applying a state-of-the-art AI-driven antenna design technique, self-adaptive Bayesian neural network surrogate model-assisted differential evolution for antenna optimization (SB-SADEA) method, the geometry parameters can be accurately determined meanwhile maintaining absorption and reflection band of the design centered at the same frequency. The fabricated prototype of the design can achieve a maximal absorption of 99.8% (-29.2 dB) and maintain an absorption over 90% in the frequency range of 2.39 to 2.42 GHz. To verify the reflection properties, a textile monopole antenna was fabricated and tested along with the reflection metasurface. A 5-dB realized gain enhancement can be achieved at 2.4 GHz with the applied metasurface. Both simulations and measurements verify the effectiveness of the proposed dual-mode metasurface design.**

***Index Terms*—textile metasurface, reconfigurable, reflection, absorption.**

I. Introduction

Much attention has been attracted to the design and application of metamaterials such as miniaturized antennas [1], radomes [2], gain-enhancement[3], metamaterial absorbers (MA) [4-6], and electromagnetic radiation shielding [7] over the past several years. Most metamaterial designs use metallic patterns on rigid substrates due to the requirement of mechanical support for the fabrication process [8, 9], which has hindered the flexibility of the design.

Flexible metamaterials are in demand for applications with conformal or wearable requirements without sacrificing electromagnetic performance[10-13]. Several studies[14-19] have proposed textile-based MA fabricated with woven conductive textiles [14, 15], and embroidery of conductive textile threads [16, 19]. Aside from textile substrate with dielectric constant close to free space, polyethylene terephthalate (PET) was integrated with textile material to function as the substrate for the design [17, 18]. Some of these works [14-18] achieve relatively good absorption with bandwidth ranging from 2.8% to 16% with a frequency center between 9 GHz to 10 GHz. Ref [19] achieves a peak absorption of 99% at 2.39 GHz with flexible embroidery techniques, meanwhile proving the practicality of designing thin textile MA functioning at a lower frequency. Ref [17, 18] presented a thorough work developing resistively loaded frequency selective surface (FSS) clad thermal blankets for enhanced radio frequency (RF) space communications. Their work further shows the significance and practical application of soft deformable textile MA.

Meanwhile, researchers are targeting the reconfigurability of the metasurfaces to expand their functionality. Most of the reported reconfigurable metasurfaces are realized by incorporating electronically controlled components, such as Positive–intrinsic–negative (PIN) diodes [20, 21], varactors [22], and Micro Electromechanical Systems (MEMS)[23]. It is worth noting that few textile metasurface designs have taken reconfigurability into account. The nature of textile materials raises the difficulty of applying surface-mounted electronic components and makes the metasurface vulnerable to deformations. These are the challenges to incorporate reconfigurability into textile metasurface design.

In this letter, a mechanically reconfigurable, dual-mode textile metasurface, with switchable reflective and absorptive modes controlled by applying a flexible carbon-coated resistive net, is presented. To the best of the authors' knowledge, this is the first time that a two-layer mechanical reconfigurable reflecting/absorbing textile metasurface structure has been proposed. The design of the two-layer structure follows an impedance-matching logic with an equivalent circuit model. The self-adaptive Bayesian neural network surrogate model-assisted differential evolution for antenna optimization (SB-SADEA) method is applied to determine the optimal matching point[24]. Full-wave simulations and experimental results are reported to support the feasibility of the proposed metamaterial.

II. Design and Analysis of the Unit Cell

The structure of one unit cell is shown in Fig. 1. In this work, felt material with a dielectric permittivity of 1.2 and a loss tangent of 0.005 is used as the substrate. The resistive net is made of carbon-coated material with conductivity of 1000 S/m (square resistance of 20 ohm/square) and thickness of 50 μm. The resistive net, conductive textile patch, felt

Manuscript received XX, 2023; revised XX; accepted XX. Date of publication XX; date of current version XX. This work was partially supported by National Natural Science Foundation of China (61801107), the Fundamental Research Funds for the Central Universities (2232022D-29), Shanghai Sailing Program (22YF1401000). *(Corresponding author: Rui Pei)*

M. Zhai, T. Zhang and R. Pei are with the College of information science and technology, Donghua University, Shanghai 201620, China, and also with Engineering Research Center of Digitized Textile and Apparel Technology, Ministry of Education, Shanghai, China. (e-mail: mlzhai@dhu.edu.cn, ruipei@dhu.edu.cn)

M. Leach, E. G. Lim, Z. Wang, and J. Wang, are with the Department of Electrical and Electronics Engineering, Xi'an Jiaotong Liverpool University, Suzhou 215123, China.

Q. Hua is with Department of Engineering and Technology, School of Computing and Engineering, University of Huddersfield, HD1 3DH Huddersfield, U.K.

M. O. Akinsolu is with the Faculty of Arts, Science and Technology, Wrexham University, LL11 2AW Wrexham, U.K.

B. Liu is with the James Watt School of Engineering, University of Glasgow, G12 8LU Glasgow, U.K. (e-mail: bo.liu@glasgow.ac.uk)

Y. Huang is with the Department of Electrical Engineering and Electronics, University of Liverpool, Liverpool L69 3BX, U.K.

Digital Object Identifier 10.1109/LAWP.2019.xxx

substrate, and conductive textile ground add up to the whole proposed Absorbing EBG (AEBG) structure. When the resistive net is removed from the structure, it functions as a Reflecting EBG (REBG). The geometrical parameters of the unit cell are **L**=58 mm, **w**=55 mm, **h**=0.5 mm, **a**=17 mm, **d**=3 mm.

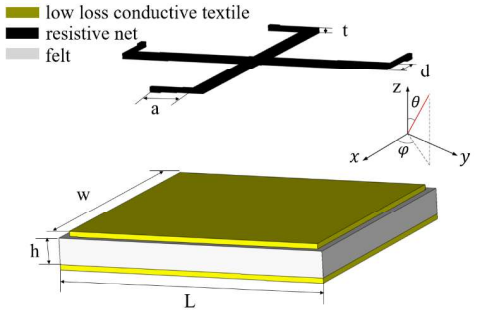

Fig. 1. The schematic view of a unit cell from the proposed structure.

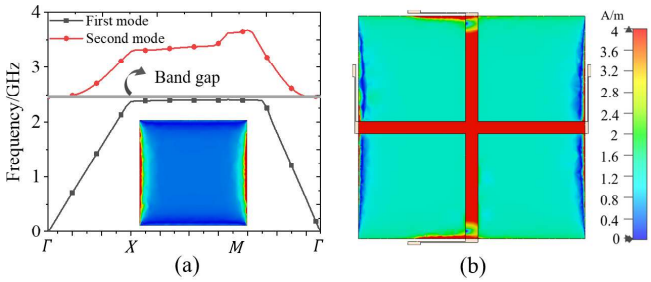

Fig. 2. (a) The dispersion diagram of the REBG. (b)Surface current distribution of the AEBG at resonance.

Planar metamaterial structures, consisting of resonators with sub-wavelength scales, are typically analyzed with dispersion diagrams[25]. The dispersion diagram of the textile EBG structure, obtained with CST eigenmode solver for surface wave propagating, is shown in Fig. 2 (a) here. The band gap between the fundamental and higher-order modes is highlighted. When considering reflection, the propagation direction of the incident wave in the unit cell analysis is set to be perpendicular to the metasurface with the electric field vector parallel to the metasurface. At this band gap frequency, the surface current concentration at the edges can be also seen in this figure. By applying the proposed resistive net above the square patches, the surface current can then be drawn to the net, which would cause energy dissipation, as shown in Fig. 2 (b).

To further verify the resistive loss on the net contributes to the majority of the energy absorption, the absolute amplitude of the reflected wave of the AEBG, REBG, AEBG without a conductive textile patch, and only the resistive net are summarized in Fig. 3. The phase of the reflected wave of the proposed REBG and a simple metal plate is also included for comparison. It can be seen that the amplitude of the reflected wave of the proposed AEBG drops to -29.2 dB at 2.4 GHz, meanwhile, for the AEBG without patch and only the resistive net cases, the structure is close to purely reflective. This shows that the energy absorption requires both the resistive net and conductive patch structure. The REBG can achieve in-phase reflection (from +90 ° to -90 °) from 2.39 GHz to 2.43 GHz, while the phase of the reflected wave of a metal plate remains close to 180 ° . These comparisons further support the logic of transforming a reflective mode to an absorptive mode by adding the resistive net.

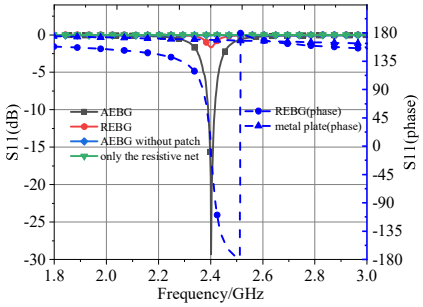

Fig. 3. The phase and amplitude of the reflected wave with different cases.

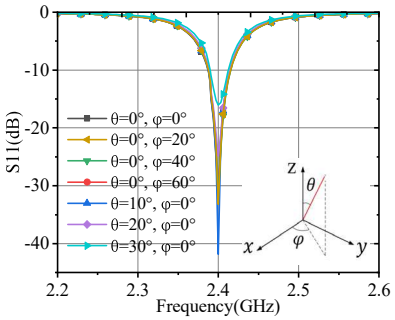

Fig. 4. Absorption for various θ angles when φ = 0° and various φ angles when θ = 0°.

Moreover, the effect of polarization and incident angle on the absorption is also investigated. Fig. 4 shows the effect on the absorption with incident angle θ varying from 0° to 30° and different polarization angle φ varying from 0° to 60°. In both cases, a relatively stable absorption can be obtained.

III. The Equivalent Circuit and Impedance Matching Analysis

An equivalent circuit and impedance matching analysis is further performed as it can elucidate the absorption mechanism and help with the parametric design.

The addition of the resistive net reduces the high impedance of the EBG to that similar to a matched load scenario, which is a value with the real part of 377 Ω and an imaginary part close to 0. The equivalent circuit model used in this analysis is shown in Fig. 5 (a). The square patches structure in the AEBG case can be modeled as conventional square patches EBG with lumped RLC elements (similar to that presented in [26]). The specific values for the components are as follows: R_1 = 16 Ω, C = 0.008 pF, L = 550 nH), and the substrate can be modeled as the impedance Z_o (Z_o = 377 Ω). When considering the AEBG as a whole, the square patches EBG structure can be considered as a current source, feeding the energy onto the resistive net. The resistive net hence can be modeled as parallel resistors in series (R_2 =520 Ω and R_3 =1500 Ω) to the equivalent current source in this case. The modification in the resistance value has little effect on the resonance frequency of the circuit, hence maintaining the same operating frequency for both the

absorption and the reflecting mode. The equivalent circuit is simulated with ADS and the result is compared with full-wave simulation performed in CST, as shown in Fig 5 (b).

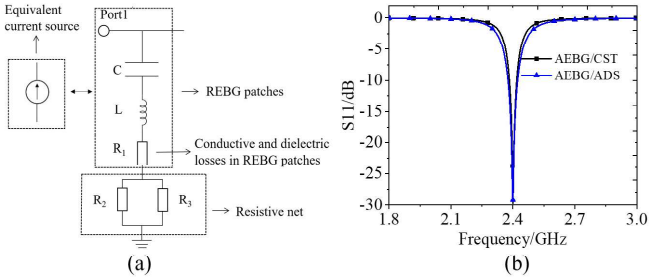

Fig. 5. The equivalent circuit model of the proposed AEBG: (a) The model; (b) S parameter comparison between circuit and full-wave simulation.

Though the equivalent circuit model presents a straightforward clarification, there is still a gap in the link between the desired resistance value and the actual geometry and material property of the resistive net. The AI-driven SB-SADEA method is a highly efficient tool to close the gap. With the material properties and a possible range for the resistive net geometry, the SB-SADEA method can search for an ideal impedance match just like in an antenna matching case. Prior to using the SB-SADEA method, the Particle Swarm Optimization (PSO) optimizer in CST Microwave Studio (MWS) was applied. SB-SADEA is the latest method in the SADEA series, which are machine learning-assisted global optimization methods for contemporary antennas. SADEA-I [27] realizes efficient global optimization of antenna structures without any initial design, and its improvements from SADEA-II to V are reviewed in [24]. The proposed unit cell is modeled and discretized in CST MWS with over 30000 Tetrahedral mesh cells. Each EM simulation costs about one minute on average on a workstation with an Intel 8-core i9-9900K 3.6 GHz CPU and 64 GB RAM. Table I compares the optimized results from the two optimization methods. After 334 EM simulations (about 6 hours), SB-SADEA obtains a design satisfying both specifications. The PSO optimizer in CST MWS takes more than 20 hours to achieve the design specifications, but the geometric constraints are not satisfied, and its results are unsuitable for fabrication. Hence, SB-SADEA is applied. It should be noted that to match the fabrication accuracy, approximations of the optimized results are used here (**a**=17 mm, **d**=3 mm).

TABLE I

SEARCH RANGES OF THE DESIGN VARIABLES AND THE OPTIMAL DESIGN BY SB-SADEA (ALL SIZES IN MM).

Results	CST-PSO Optimum	SB-SADEA Optimum
a	8.8	17.2
d	25.6	3.1
Bandwidth (GHz)	2.38-2.41	2.39-2.42
Time (hour)	20	6

*The constraint for the value of a and d: a ⩾ d, a ⩽ d/2 +27.5.

IV. FABRICATION AND EXPERIMENTAL RESULTS

A metasurface prototype with 12-by-12 unit cells is fabricated, the photo of which is included in Fig. 6. Wool blend felt material is used as the substrate material. The dielectric constant and loss tangent are measured with the waveguide transmission line method. The material of patches and ground is a conductive textile with a surface conductivity of 8×10^5 S/m (measured with an HPS2661 precision four-probe resistivity measurement system and verified with a square patch antenna in a reverberation chamber). The conductivity of the resistive net material is 1000 S/m, which is also measured with HPS2661.

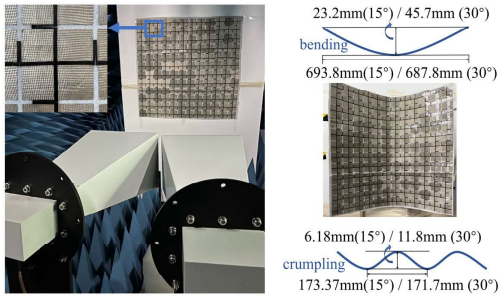

Fig. 6. (a) The measurement setup for the absorption. (b) Simplified schematic of bending and crumpling cases.

The reflection amplitude of the fabricated prototype is measured in an anechoic chamber with a set of standard gain horn antennas and an Agilent N5230C network analyzer. The measurement setup is shown in Fig. 6. The measured results generally matched the simulated results, as shown in Fig. 7. Fig. 7 (a) shows the simulation and measured results of the flat AEBG and crumpling AEBG, and Fig. 7 (b) shows the simulation and measured results of flat AEBG and bending AEBG. However, the 90% absorption band shifts slightly towards lower frequencies but the maximal absorption remains stable. It is mainly due to the inaccuracy in the manufacturing process and the limitation in the experiment setup. Meanwhile, there is a second absorption peak at 2.1 GHz or 2.2 GHz for some crumpling and bending cases, this is mainly because the resonances with shifted frequency centers happen on partial sections of the metasurface under deformation. For EBG structures formed by conductive textile square patch arrays, the deformation changes the gap between square patches and the thickness of the substrate; hence changing the equivalent capacitance of partial sections, resulting in resonances (absorption peaks) frequency shifts.

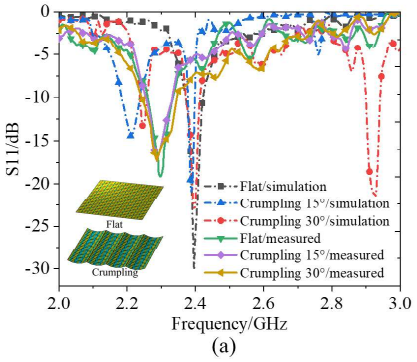

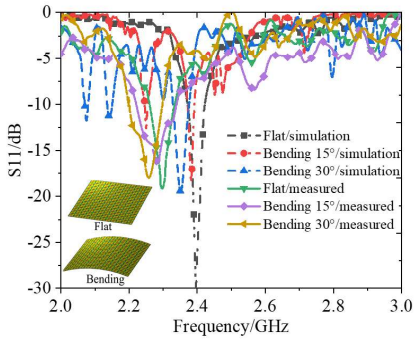

(b)

Fig. 7. Comparison of the measured and simulated amplitudes of the reflected wave on different curvatures (a) flat and crumpling. (b) flat and bending

The performance of the REBG is evaluated by applying a textile-based monopole antenna on top of the surface. As shown in Fig. 3, the zero-degree phase of the reflected wave center of the REBG is tuned to 2.4 GHz. This means that the reflected EM waves will propagate in the same phase as the incident wave and form a stronger main lobe, which helps concentrate radiated energy and increases the gain of the antenna at 2.4 GHz. This is the intended application for the textile REBG. Hence, the performance is tested with a monopole antenna placed on top of the REBG. The radiation patterns for the antenna alone and the antenna loaded with REBG at 2.4 GHz are shown in Fig. 8. It can be seen from the results that the maximal gain of the antenna loaded with REBG is increased by a level of 5 dB, proving the effectiveness of the reflecting mode of this design.

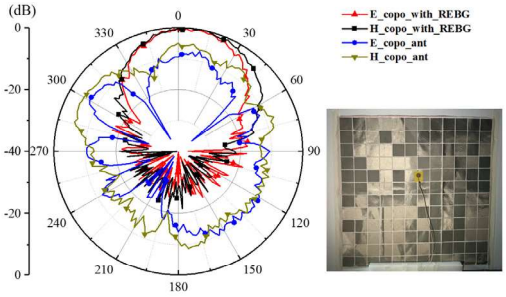

Fig. 8. 2D radiation pattern of the antenna with/without the REBG.

To further demonstrate the novelty of the proposed method, the materials, absorption, operating frequency, polarization insensitivity, incident angle insensitivity, and reconfigurability of the proposed design are compared with previously reported works in Table II. It can be seen that few textile metasurface designs have taken reconfigurability into account and the proposed design has not only polarization insensitivity but also incident angle insensitivity. More importantly, it has reconfigurability without electronically controlled components, which means that the preparation process of this design is relatively simple and low-cost. This design presents excellent absorption for the absorbing mode.

TABLE II

COMPARISON OF OUR WORK AND RELATED DESIGNS.

Ref.	Materials	Absorption	Frequency/GHz	PI	II	Reconfigurability
[14]	Felt+ Metalized nylon fabric	90.1%, 92.8%	9, 9.85	Yes	Yes	No
[15]	Double-sided bonding tape+ Fabric+ Silver	94.25%	9.69	Yes	Yes	No
[16]	Cotton+ Embroidered metal yarn	98.39%	10.46	No	No	No
[18]	Polyethylene terephthalate sheet+ Foil	over 99%	9.91	No	No	No
[19]	Scuba knitting fabric+ Embroidered metal yarn	99%	2.39	No	Yes	No
[21]	FR4+Metal+PIN	93.51%	6.93	Yes	No	PIN
[22]	Nylon screws+Spacers+Resistors+Varactors	over 90%	2.4-6.58	No	Yes	Varactors
[28]	Water+ Low-permittivity material+Metal	over 90%	6.2-19	No	No	The temperature of the water
This work	Felt+ Conductive textile+ Carbon-coated resistive film	99.8%	2.4	Yes	Yes	Carbon-coated resistive film

*Polarization insensitivity (PI), incident angle insensitivity (II).

V. CONCLUSION

In this letter, a textile-based reflecting/absorbing dual-mode metasurface design is proposed. Operating at the same frequency band, the metasurface can either function as an EBG reflector for a linear polarized antenna, or a thin absorber, simply by removing or attaching the resistive layer. The underlying principle of the design is analyzed in terms of the dispersion diagram, current distribution, and an equivalent circuit for impedance matching. Thanks to the SB-SADEA method, the geometry parameters for the structure can be obtained efficiently without excessive parament sweeping. The design has been fabricated to demonstrate the practicality of the metasurface unit. The measured results are in good agreement with the simulations. The concept of this design could be extended to other frequency ranges, and it has potential applications in conformal scenarios due to its textile-based nature and relatively stable performance under deformation.

ACKNOWLEDGMENT

The authors would like to thank CST AG for providing the CST Studio Suite Electromagnetic Simulation Software package under the China Key University Promotion Program and Suzhou Municipal Key Lab for Wireless Broadband Access Technologies in the Department of Electrical Engineering, Xi'an Jiaotong Liverpool University, Suzhou, China, for research facilities. The authors would also like to thank the company Nake New Materials for providing carbon-coated resistive net materials.

REFERENCES

[1] T. Yue, Z. H. Jiang, A. H. Panaretos, and D. H. Werner, "A Compact Dual-Band Antenna Enabled by a Complementary Split-Ring Resonator-Loaded Metasurface," *IEEE Transactions on Antennas and Propagation,* vol. 65, no. 12, pp. 6878-6888, 2017.

[2] W. Wu, X. Liu, K. Cui, Y. Ma, and Y. Yuan, "An Ultrathin and Polarization-Insensitive Frequency Selective Surface at Ka-Band," *IEEE Antennas and Wireless Propagation Letters,* vol. 17, no. 1, pp. 74-77, 2018.

[3] A. Bousselmi, A. Gharsallah, and T. P. Vuong, "Improving the Gain of a Multiband Antenna by Adding an AMC Metasurface," in *2023 Photonics & Electromagnetics Research Symposium (PIERS)*, 2023, pp. 2178-2183.

[4] Y. Kato, S. Morita, H. Shiomi, and A. Sanada, "Ultrathin Perfect Absorbers for Normal Incident Waves Using Dirac Cone Metasurfaces With Critical External Coupling," *IEEE Microwave and Wireless Components Letters,* vol. 30, no. 4, pp. 383-386, 2020.

[5] G. G. Machado, R. Cahill, V. Fusco, and G. Conway, "Comparison of FSS Topologies for Maximising the Bandwidth of Ultra-Thin Microwave Absorbers," in *2019 13th European Conference on Antennas and Propagation (EuCAP)*, 2019, pp. 1-5.

[6] G. G. Machado, R. Cahill, V. Fusco, and G. Conway, "Resistively loaded ultra-thin FSS absorbers for radio-frequency enhancement of spacecraft thermal blankets," *IET Microwaves, Antennas & Propagation,* vol. 13, no. 11, pp. 1928-1933, 2019.

[7] M. Nauman, R. Saleem, A. K. Rashid, and M. F. Shafique, "A Miniaturized Flexible Frequency Selective Surface for X-Band Applications," *IEEE Transactions on Electromagnetic Compatibility,* vol. 58, no. 2, pp. 419-428, 2016.

[8] A. Haridas, N. J. J, M. Babu, and O. R. M, "Wide Bandwidth Angular Insensitive Metamaterial Absorber for X Band Application," in *2022 IEEE Delhi Section Conference (DELCON)*, 2022, pp. 1-5.

[9] A. Androne, R. D. Tamas, and S. Tasu, "Influence of the Substrate Material on the Radar Cross Section of Square Loop Unit Cells for Frequency Selective Surfaces," in *2020 International Workshop on Antenna Technology (iWAT)*, 2020, pp. 1-4.

[10] A. E. Butler and C. Argyropoulos, "Mechanically Tunable Broadband Omnidirectional Infrared Absorption by Dielectric Metasurfaces," in *2022 IEEE International Symposium on Antennas and Propagation and USNC-URSI Radio Science Meeting (AP-S/URSI)*, 2022, pp. 677-678.

[11] S. Ghosh and S. Lim, "A Multifunctional Reconfigurable Frequency-Selective Surface Using Liquid-Metal Alloy," *IEEE Transactions on Antennas and Propagation,* vol. 66, no. 9, pp. 4953-4957, 2018.

[12] Y. Fang, K. Pan, T. Leng, H. H. Ouslimani, K. S. Novoselov, and Z. Hu, "Controlling Graphene Sheet Resistance for Broadband Printable and Flexible Artificial Magnetic Conductor-Based Microwave Radar Absorber Applications," *IEEE Transactions on Antennas and Propagation,* vol. 69, no. 12, pp. 8503-8511, 2021.

[13] K. S. Umadevi, S. K. Simon, S. P. Chakyar, J. Andrews, and V. P. Joseph, "Wide Band Microwave Absorber using Flexible Broadside Coupled Split Ring Resonator Metamaterial Structure," in *2019 Thirteenth International Congress on Artificial Materials for Novel Wave Phenomena (Metamaterials)*, 2019, pp. X-453-X-455.

[14] J. Tak and J. Choi, "A Wearable Metamaterial Microwave Absorber," *IEEE Antennas and Wireless Propagation Letters,* vol. 16, pp. 784-787, 2017.

[15] E. Erdem and A. H. Yuzer, "Textile-based 3D metamaterial absorber design for X-band application," *Waves in Random and Complex Media,* pp. 1-10, 2022.

[16] O. Almirall, R. Fernández-García, and I. Gil, "Wearable metamaterial for electromagnetic radiation shielding," *The Journal of The Textile Institute,* vol. 113, no. 8, pp. 1586-1594, 2022/07/25 2022.

[17] G. G. Machado, R. Cahill, V. Fusco, and G. Conway, "Resistively Loaded FSS Clad Thermal Blankets for Enhanced RF Space Communications," in *2019 International Conference on Electromagnetics in Advanced Applications (ICEAA)*, 2019, pp. 0048-0052.

[18] G. G. Machado, R. Cahill, V. Fusco, and G. A. Conway, "Suppression of Antenna Backscatter on a Nanosat Using a Resistively Loaded FSS Absorber," *IEEE Antennas and Wireless Propagation Letters,* vol. 18, no. 12, pp. 2607-2611, 2019.

[19] Y. Yang, J. Wang, C. Song, R. Pei, J. M. Purushothama, and Y. Zhang, "Electromagnetic shielding using flexible embroidery metamaterial absorbers: Design, analysis and experiments," *Materials & Design,* vol. 222, p. 111079, 2022/10/01/ 2022.

[20] R. Zhao, L. Shao, and W. Zhu, "Switchable metamaterial absorber and reflector using PIN diodes," in *2019 International Conference on Microwave and Millimeter Wave Technology (ICMMT)*, 2019, pp. 1-3.

[21] P. M. Sainadh, A. Sharma, and S. Ghosh, "Polarization-Insensitive Absorptive/Transmissive Reconfigurable Frequency Selective Surface With Embedded Biasing," *IEEE Antennas and Wireless Propagation Letters,* vol. 22, no. 1, pp. 164-168, 2023.

[22] Y. Wang, S. S. Qi, Z. Shen, and W. Wu, "Tunable Frequency-Selective Rasorber Based on Varactor-Embedded Square-Loop Array," *IEEE Access,* vol. 7, pp. 115552-115559, 2019.

[23] M. Chung, H. Jeong, Y. K. Kim, S. Lim, and C. W. Baek, "Design and Fabrication of Millimeter-Wave Frequency-Tunable Metamaterial Absorber Using MEMS Cantilever Actuators," (in eng), *Micromachines (Basel),* vol. 13, no. 8, Aug 20 2022.

[24] Y. Liu *et al.*, "An Efficient Method for Antenna Design Based on a Self-Adaptive Bayesian Neural Network-Assisted Global Optimization Technique," *IEEE Transactions on Antennas and Propagation,* vol. 70, no. 12, pp. 11375-11388, 2022.

[25] F. Yang and Y. Rahmat-Samii, *Electromagnetic Band Gap Structures in Antenna Engineering* (The Cambridge RF and Microwave Engineering Series). Cambridge: Cambridge University Press, 2008.

[26] A. Bhardwaj, A. Sharma, K. V. Srivastava, and S. A. Ramakrishna, "Polarization Insensitive Resistive Ink based Conformal Absorber for S and C bands," in *2019 IEEE Indian Conference on Antennas and Propogation (InCAP)*, 2019, pp. 1-4.

[27] B. Liu, H. Aliakbarian, Z. Ma, G. A. E. Vandenbosch, G. Gielen, and P. Excell, "An Efficient Method for Antenna Design Optimization Based on Evolutionary Computation and Machine Learning Techniques," *IEEE Transactions on Antennas and Propagation,* vol. 62, no. 1, pp. 7-18, 2014.

[28] Y. Pang *et al.*, "Thermally tunable water-substrate broadband metamaterial absorbers," *Applied Physics Letters,* vol. 110, no. 10, 2017.